REGULAR PAPERS

Local pulse wave velocity estimated from small vibrations measured ultrasonically at multiple points on the arterial wall

Japanese Journal of Applied Physics **57**, 07LF14 (2018)
https://doi.org/10.7567/JJAP.57.07LF14

REGULAR PAPER

Local pulse wave velocity estimated from small vibrations measured ultrasonically at multiple points on the arterial wall

Mika Ito[1], Mototaka Arakawa[1,2], and Hiroshi Kanai[2,1*]

[1]*Graduate School of Biomedical Engineering, Tohoku University, Sendai 980-8579, Japan*
[2]*Graduate School of Engineering, Tohoku University, Sendai 980-8579, Japan*

*E-mail: kanai@ecei.tohoku.ac.jp

Received November 6, 2017; accepted February 4, 2018; published online June 11, 2018

Pulse wave velocity (PWV) is used as a diagnostic criterion for arteriosclerosis, a major cause of heart disease and cerebrovascular disease. However, there are several problems with conventional PWV measurement techniques. One is that a pulse wave is assumed to only have an incident component propagating at a constant speed from the heart to the femoral artery, and another is that PWV is only determined from a characteristic time such as the rise time of the blood pressure waveform. In this study, we noninvasively measured the velocity waveform of small vibrations at multiple points on the carotid arterial wall using ultrasound. Local PWV was determined by analyzing the phase component of the velocity waveform by the least squares method. This method allowed measurement of the time change of the PWV at approximately the arrival time of the pulse wave, which discriminates the period when the reflected component is not contaminated.

1. Introduction

The arterial wall consists of three layers: (1) the intima, which is the innermost thin layer; (2) the thick media, which contains elastin, smooth muscle, and collagen; and (3) the outermost adventitia, which is predominantly made of stiff collagenous fibers. In the media, collagen is the stiffest wall constituent with elastic moduli of 3–100 MPa.[1)] The elastic moduli of elastin and smooth muscle are 6×10^2 and $(0.1–2.5) \times 10^2$ kPa, respectively.[2)]

Clinical observations suggest that the ratio of nondistensible components (collagen and basement membrane) to the distensible components (smooth muscle and elastin) changes markedly with aging and the progression of atherosclerosis, which structurally affects the elastic behavior of the arterial wall.[3,4)] In particular, in the early stage of atherosclerosis, the cholesterol ester content of the aortae significantly affects the dynamic Young's modulus of the aorta.[5)]

The elasticity or viscoelasticity of the arterial wall has been measured in extracted blood vessels or exposed vessels in animal experiments.[2,6–12)] Alternatively, changes in the stiffness of human arteries can be assessed by the noninvasive measurement of displacement of the arterial wall using an ultrasonic phase-locked echo tracking system.[13,14)] However, in those studies, the pulse pressure, which is essential for viscoelasticity estimation, was measured at the brachial artery.

As a noninvasive clinical method for evaluating arterial elasticity, pulse wave velocity (PWV) has been used for the diagnosis of arteriosclerosis for more than 100 years.[15–17)] On the basis of wave transmission theories, PWV is determined using the well-known Moens–Korteweg formula:

$$PWV = \sqrt{\frac{E_\theta h}{2\rho r_0}}, \tag{1}$$

where E_θ is the Young's modulus of elasticity in the circumferential direction of the arterial wall, r_0 and h are the internal radius and thickness of the arterial vessel, respectively, and ρ is the density of blood. The assumptions for the Moens–Korteweg equation are that the artery has a thin wall (i.e., $h/2r_0$ is sufficiently small) and is filled with an incompressible inviscid liquid. From the noninvasive measurement of the PWV in Eq. (1), the elasticity of the arterial wall is evaluated.

More exact solutions of pulse wave transmission have also been reported.[15,18,19)] The full correction equation was described by Bergel,[2,6)] and its effective simplification is

$$PWV(E_\theta) = \sqrt{\frac{1}{1-\sigma^2} \cdot \frac{E_\theta h}{2\rho r_0}}, \tag{2}$$

where σ is the Poisson's ratio of the arterial wall. Using a Poisson's ratio of 0.5 results in a derived velocity $PWV(E_\theta)$ that is higher than the PWV in Eq. (1) by a factor of $\sqrt{4/3} \approx 1.15$. Noninvasive evaluation of PWV from the elastic modulus E_θ uses the Moens–Korteweg equation shown in Eq. (1) or (2); the latter is more accurate when the viscoelastic effects are included.[20)]

In numerous studies, various methods have been developed for measuring the PWV of extracted or exposed arteries in anesthetized animals. These are divided into the following four categories.

1. Wave-front velocity measurement using a pair of catheter-tip manometers[21)] or the systolic foot-to-foot velocity measurement using pressure pulses by in vivo aortic catheterization.[8)] For the exposed arteries, the phase velocity of the harmonic components of small artificially generated pressure waves was measured both in the downstream and upstream directions.[22,23)]
2. Estimation of the PWV in Eq. (1) based on the measurement of the dynamic elastic modulus detected from the oscillatory stress–strain relationships at each frequency.[6,8,12)]
3. Frequency-dependent phase velocity determination from the propagation constant (γ) based on the theory of transmission lines using the Fourier spectra of measured pressure and blood flow, or pressures measured at three or four points in an arterial segment where forward and reflected waves exist.[24–35)] Complex characteristic impedance and local reflection coefficients were also determined.[36–41)]
4. The phase velocities in the artery were calculated from the Fourier spectra of simultaneous measurements of pressure at two sites.[42,43)]

All of these methods were applied to extracted arteries in vitro, or exposed or unexposed arteries of anesthetized animals or patients in vivo using invasive manometers.

Alternatively, some noninvasive methods of in vivo measurement of PWV have been developed, including the assessment of foot-to-foot velocity from a pair of pressure waves measured on the skin surface,[44–46] from a pair of displacement components,[47–50] or from velocity components[51,52] in the radial direction of the arterial wall using two-channel echo tracking devices, or from blood flow speed at two points using ultrasound.[53–57] In all of these noninvasive methods, the pressure wave near the skin surface, wall displacement, wall velocity, blood flow, and radiated sound are measured at two points along the vessel wall, and the delay time in the transmission of the foot of pulse waveforms (i.e., the point showing the sharpest change in the wave) is determined. PWV is determined only at the beginning of the ejection period T_E.

However, to the best of our knowledge, there are no reports of measurement of PWV at periods other than T_E during one cardiac cycle. As described above, as the arterial wall exhibits nonlinear characteristics in the stress–strain relationship, PWV changes during one cardiac cycle because of the change in inner pressure. Furthermore, the velocity dispersion in PWV in vivo has not been reported. The measurable frequency of typical PWV components is less than 20 Hz. Thus, the wavelength at 20 Hz is approximately 25–50 cm, as typical PWVs in humans are approximately 5–10 m/s. In the presence of both a forward transmission wave and a backward reflection wave, these two components cannot be separated in the time domain. At the beginning of the ejection period T_E, only the forward transmission wave exists. Thus, PWV is only measured noninvasively at this time.

In conventional measurement methods, blood pressure is measured at two points. PWV is calculated from the difference in the rise time of blood pressure waveforms and the distance between two points, as in the case of the carotid-femoral PWV method,[47,58] by which PWV is calculated from the carotid artery to the femoral artery, and the brachial-ankle PWV method, by which PWV is calculated between the brachial artery and the ankle. However, these methods have the following problems.

1. The measurement region is as wide as several tens of centimeters, such as between the carotid artery and the femoral artery or between the brachial artery and the ankle. Although PWV increases as much as in peripheral blood vessels,[59] this effect is not considered in PWV measurements using conventional methods, but PWV is rather calculated from the average velocity over a wide region (from the central artery to peripheral blood vessels).
2. The pulse wave generated with the heart beat propagates toward the periphery of the arterial wall and is reflected at vascular bifurcations and peripheral vessels.[60] Nevertheless, PWV is calculated on the assumption that the pulse wave has only an incident component.

Therefore, local lesions on the order of several millimeters to tens of millimeters may not be evaluated correctly.[61,62] Moreover, Young's modulus increases as arteriosclerosis progresses, while PWV increases in proportion to the square root of Young's modulus. As arteriosclerosis progresses, the pulse wave reflected from the peripheral bifurcations returns earlier. Thus, the incident component of the pulse wave interferes with the reflected component.

We previously reported the local PWV calculation method using high-frame-rate ultrasound for in vivo measurement of the carotid artery.[63] However, PWV was calculated only at the peak time of the acceleration waveforms of small vibrations on the arterial wall, and the reflected pulse wave was not observed in all subjects. In this study, we noninvasively measured the velocity waveforms of small vibrations at multiple points on the arterial wall using ultrasound, and calculated the change in time of local PWV by analyzing the phase waveforms of the velocity signals. By calculating the change in time of the local PWV, the incident and reflected components of the pulse wave were observed, and the period including only the incident component of the pulse wave and that including only the reflected component of the pulse wave were separately extracted for all subjects. Moreover, the propagation of mechanical vibration accompanying the opening of the aortic valve was observed.

2. Experimental methods

2.1 Tracking of the arterial wall using the phased-tracking method

In this study, we measured small vibrations on the arterial wall as velocity waveforms using the phased-tracking method.[64,65] In this method, the average velocity during the pulse transmission interval ΔT is obtained as the waveform $v(t)$ from the phase difference $\Delta\theta(x;t)$ during the period ΔT as follows:

$$\hat{v}\left(t+\frac{\Delta T}{2}\right)=\frac{\Delta x(t)}{\Delta T}=c_0\cdot\frac{\Delta\theta(x;t)}{4\pi f_0\Delta T}, \tag{3}$$

where c_0 is the velocity of the ultrasound, $\Delta x(t)$ is the displacement of an object during the period ΔT, and f_0 is the frequency of the ultrasound.

2.2 Calculation of PWV by the least squares method

The analytic signal $a(n)$ of the velocity waveform $v(n)$ in Eq. (3) on the arterial wall was calculated using the Hilbert transform, where n is a frame number. The phase waveform $\theta(n)$ of the analytic signal $a(n)$ was discontinuous because the range of the phase $\theta(n)$ was $-\pi<\theta(n)\leq\pi$. To obtain continuous waveforms, the phase unwrapping process was applied. Then, the line with similar phase values from the first beam to the last beam was determined by the least squares method to estimate the component that propagates with PWV as follows. First, when we assume a value of PWV, the arrival time $t_{m,n,PWV}$ of the pulse wave on the mth ultrasound beam is given by

$$t_{m,n,PWV}=\frac{\Delta d\cdot m}{PWV}+\Delta T\cdot n\quad(m=0,1,\ldots,M), \tag{4}$$

where Δd is the interval beams, ΔT is the sampling interval of the velocity waveform $v(t)$, and $\Delta T\cdot n$ is the base time set on the 0th beam of the selected nth frame. The instantaneous phase value $\theta_m(t_{m,n,PWV})$ at the time $t_{m,n,PWV}$ for the mth beam obtained from the analytic signal is described above.

Second, the pulse wave velocity $PWV(\Delta T\cdot n)$ at a time $\Delta T\cdot n$ is determined by minimizing the following root of the variance, $\alpha(PWV,n)$, of $\theta_m(t_{m,n+k,PWV})$ along the straight line

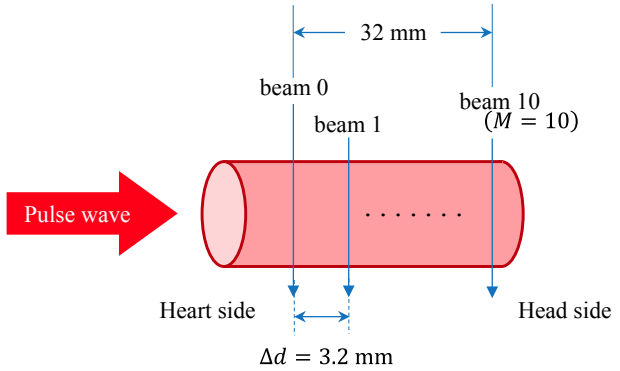

Fig. 1. (Color online) Schematic diagram of the in vivo measurement.

determined by Eq. (4) in all beams ($m = 0, 1, \ldots, M$) related to $\Delta T \cdot n$:

$$\alpha(PWV, n) = \frac{1}{3}\sum_{k=-1}^{1}\left(\frac{1}{M+1}\sum_{m=0}^{M}|\theta_m(t_{m,n+k,PWV}) - \overline{\theta_k}|^2\right), \quad (5)$$

where $\overline{\theta_k}$ is the mean value defined by

$$\overline{\theta_k} = \frac{1}{M+1}\sum_{m=0}^{M}\theta_m(t_{m,n+k,PWV}), \quad (6)$$

and $(M + 1)$ shows the number of ultrasound beams.

2.3 Experimental setting

In vivo measurements were performed using an ultrasonic diagnostic device (Hitachi-Aloka ProSound F75) with a 6.0 MHz linear probe (Hitachi-Aloka UST-5415). Radio frequency signals were acquired in the carotid artery of three healthy male subjects (A, B, and C). The sampling frequency was 40 MHz, and the resolution in the axial direction was 38.5 µm. The 11 ultrasound beams (beam number $m = 0, 1, \ldots, 10$) were set in the longitudinal direction along the arterial wall with intervals of $\Delta d = 3.2$ mm, and the velocity waveform of a small vibration for each beam was measured at the boundary between the media and the adventitia on the posterior wall of the carotid artery for 4 s. The frame rate was $1/\Delta T = 521$ Hz. The phase components $\theta(n)$ were interpolated in advance by the sinc function at seven points between the sampling interval of ΔT. Figure 1 shows a schematic diagram of the in vivo measurement.

3. Results and discussion

3.1 Results of subject A

Figure 2 shows the B-mode image of subject A (23-year-old healthy male). Figure 3 shows the velocity waveforms of small vibrations on the arterial wall, which were obtained on six beams $\{v_m(t)\}$ ($m = 0, 2, 4, 6, 8, 10$). All velocity waveforms $\{v_m(t)\}$ showed two negative peaks immediately after aortic valve opening, and two positive peaks immediately after aortic valve closing. First, we focused on the time when the velocity waveforms of the small vibrations peaked on each beam. When we assumed that the PWV was constant regardless of the measurement position, some pulse waves were found to propagate, as shown by green lines, immediately after the first heart sound in the phonocardiogram (PCG); the incident and reflected components of the pulse wave were discriminated by the positive and negative gradients of the lines, respectively. From the gradient of each green line, the velocities of the first incident pulse wave

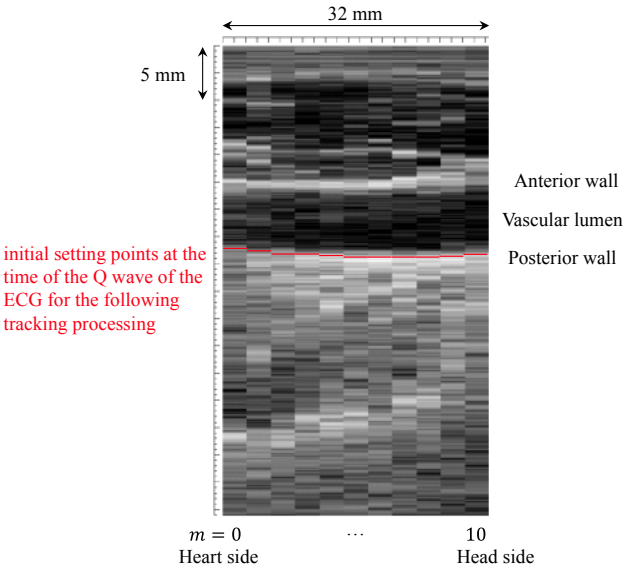

Fig. 2. (Color online) B-mode of subject A.

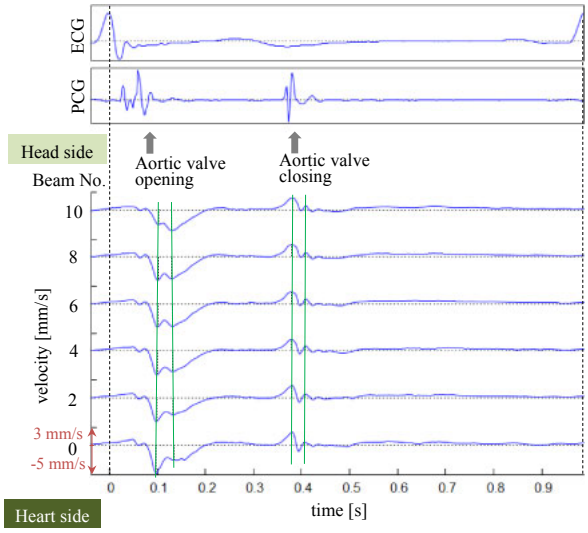

Fig. 3. (Color online) Velocity waveforms of small vibrations on the arterial wall for even beams ($m = 0, 2, 4, 6, 8, 10$), ECG, and PCG of subject A.

and the second reflected pulse wave were 5.3 and −8.0 m/s, respectively.

The analytic signals of velocity waveforms were obtained using the Hilbert transform, and phase unwrapping was applied to the phase waveforms of the analytic signals to obtain continuous phase waveforms. Figure 4 shows the color maps of the phase before and after the phase unwrapping and the electrocardiogram (ECG) and PCG. Figure 5(e) shows the PWV determined by applying the least squares method for Eq. (4) to the period immediately after the first heart sound. We considered that there was almost no vibration on the arterial wall during the period when the root mean square (RMS) of velocity was less than 1 mm/s. Thus, we determined PWV until 0.25 s after the R-wave of the ECG, and focused on the time immediately after the first heart sound. At the time when the velocity waveforms of the small vibrations on the arterial wall had two peaks immediately after the first heart sound, the incident component of the pulse wave was calculated as approx-

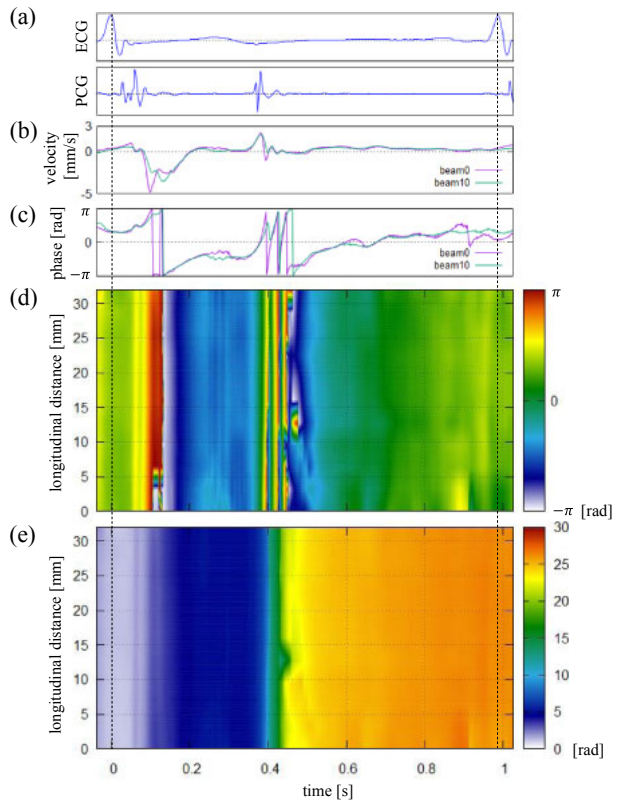

Fig. 4. (Color online) Result of the phase unwrapping of subject A. (a) ECG and PCG. (b) Velocity waveforms of small vibrations on the arterial wall of beam 0 and beam 10. (c) Phase waveforms of the velocity of beam 0 and beam 10. (d) Color map of phase before the phase unwrapping. (e) Color map of phase after the phase unwrapping.

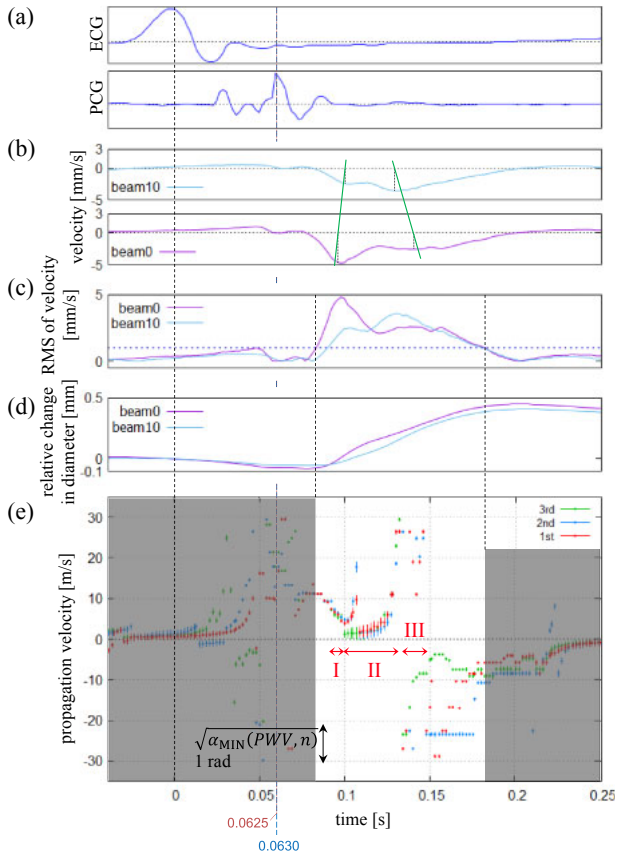

Fig. 5. (Color online) (a) ECG and PCG of subject A. (b) Velocity waveforms of small vibrations on the arterial wall of beam 0 and beam 10. (c) RMS of velocity waveforms small vibrations on the arterial wall of beam 0 and beam 10. (d) Relative changes in the inner diameter of the blood vessel. (e) Pulse wave velocity of subject A determined by the least squares method.

imately 5.0 m/s at around 0.10 s, and the reflected component of the pulse wave was calculated as approximately −8.0 m/s at around 0.14 s. These results correspond to those shown in Fig. 3.

Moreover, a component of approximately 10 m/s was obtained at 0.08 s immediately before the arrival of the incident component of the pulse wave, which is related to the propagation of mechanical vibration accompanied by the opening of the aortic valve as follows. Since the distance from the heart to the common carotid artery was roughly 17.5 cm, the times at which the mechanical vibration at 10 m/s and the incident component of the pulse wave at 5.0 m/s occurred were calculated as 62.5 and 63.0 ms after the R-wave of the ECG, respectively. As shown by the broken and dotted lines in Fig. 5(a), the PCG showed a large peak at the time when these two propagation components occurred. Thus, these phenomena show that the pulse wave starts to propagate with the opening of the aortic valve from the heart to the common carotid artery by accompanying the mechanical vibration. By comparing the results at three heartbeats shown in Fig. 5(e), the velocities estimated were similar for the incident component of the pulse wave and the mechanical vibration, while those for the reflected component of the pulse wave were different.

The rise time of the relative change in the inner diameter of the blood vessel in Fig. 5(d), at which the *PWV* was measured using the conventional method, corresponded to the time at which the propagation component was converted from the mechanical vibration to the incident component of the pulse wave. Thus, the *PWV* at the rise time of the relative change in the inner diameter of the blood vessel waveform (approximately 8.0 m/s) in Fig. 5(d) was slightly higher than that of the incident component of the pulse wave. By the conventional technique, the risk of arteriosclerosis is considered high if the PWV is ≥14 m/s measured by the brachial-ankle PWV method,[66] or if the PWV is ≥10 m/s measured by the carotid-femoral PWV method.[67] The velocity of the incident pulse wave component estimated in the present study was within the normal range based on these diagnostic criteria.

3.2 Results of subject B

Figure 6 shows the velocity waveforms that were obtained on six beams of subject B (23-year-old healthy male). The velocities of the first incident pulse wave and the second reflected pulse wave were obtained at 5.3 and −10.7 m/s, respectively. At the same time, the incident and reflected components of the pulse wave were calculated by the least squares method as approximately 5.7 m/s around 0.14 s and −11 m/s around 0.17 s, respectively, in Fig. 7(e). These results also corresponded to the results in Fig. 6. A component of the mechanical vibration was observed as approximately 10 m/s at around 0.13 s. Since the distance from the heart to the common carotid artery was roughly 17.5 cm, the times at which the mechanical vibration at 10 m/s and the incident component of the pulse wave at 5.7 m/s occurred were calculated as 110 and 109 ms after the R-wave of the ECG, respectively. As shown by the broken and dotted

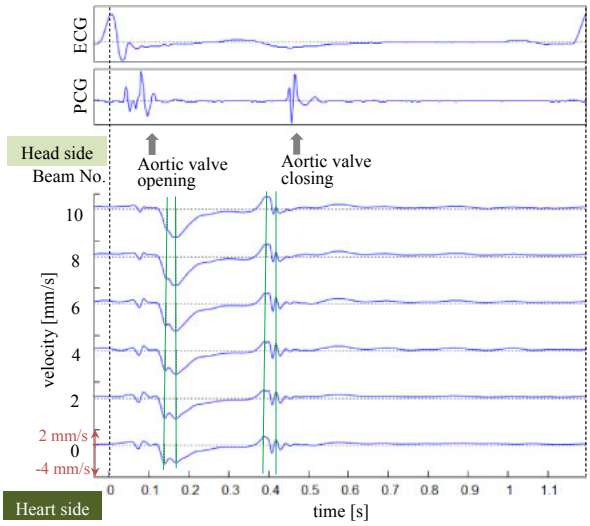

Fig. 6. (Color online) Velocity waveforms of small vibrations on the arterial wall for even beams ($m = 0, 2, 4, 6, 8, 10$), ECG, and PCG of subject B.

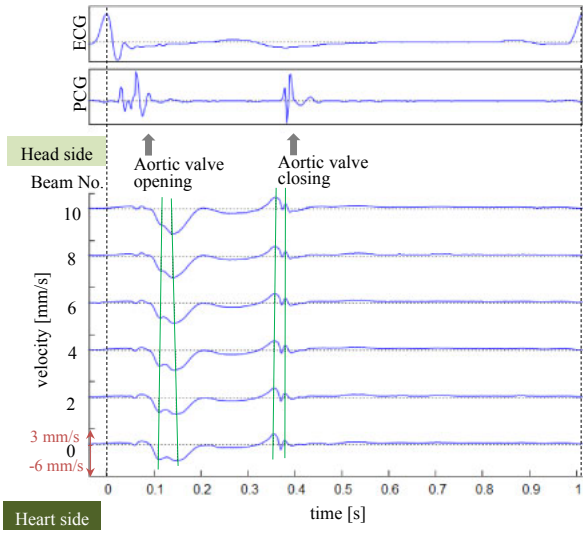

Fig. 8. (Color online) Velocity waveforms of small vibrations on the arterial wall for even beams ($m = 0, 2, 4, 6, 8, 10$), ECG, and PCG of subject C.

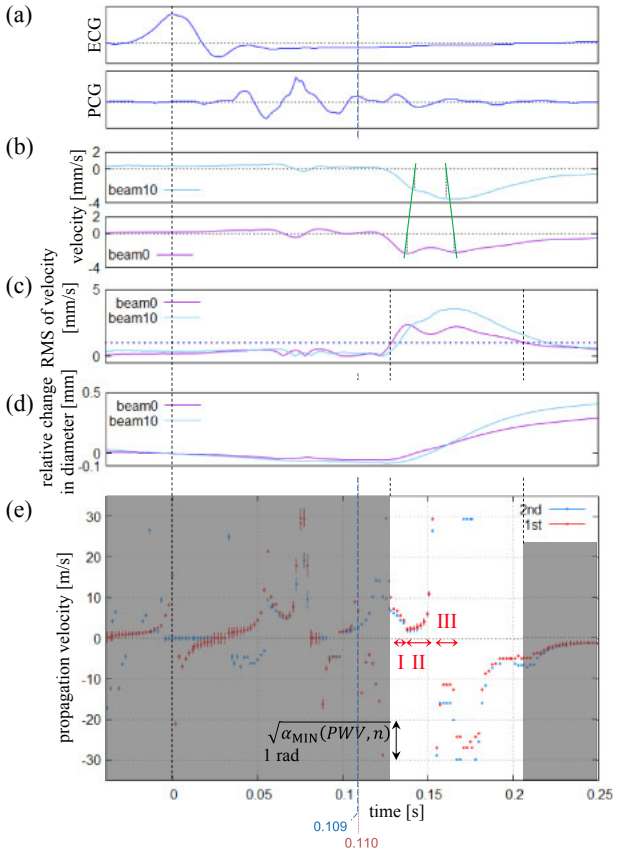

Fig. 7. (Color online) (a) ECG and PCG of subject B. (b) Velocity waveforms of small vibrations on the arterial wall of beam 0 and beam 10. (c) RMS of velocity waveforms of small vibrations on the arterial wall of beam 0 and beam 10. (d) Relative changes in the inner diameter of the blood vessel. (e) Pulse wave velocity of subject B determined by the least squares method.

lines in Fig. 7(a), the PCG showed a peak at the time when these two propagation components occurred. By comparing the results between two heartbeats as shown in Fig. 7(e), the velocities estimated were similar for the incident component of the pulse wave and the mechanical vibration, while those for the reflected component of the pulse wave were different.

The rise time of the relative change in the inner diameter of the blood vessel in Fig. 7(d) also corresponded to the time at which the propagation component was converted from the mechanical vibration to the incident component of the pulse wave, while the *PWV* at that time was slightly higher than the incident component of the pulse wave. On the basis of the diagnostic criteria of the conventional methods, the velocity of the incident pulse wave component estimated in the present study was within the normal range.

3.3 Results of subject C

Figure 8 shows the velocity waveforms that were obtained on six beams of subject C (24-year-old healthy male). The velocities of the first incident pulse wave and second reflected pulse wave were 5.6 and −7.1 m/s, respectively. At the same time, the incident and reflected components of the pulse wave were calculated by the least squares method as approximately 5.7 m/s at around 0.11 s and approximately −7.0 m/s at around 0.14 s, respectively, in Fig. 9(e). These results also corresponded to the results in Fig. 8. A component of the mechanical vibration was observed as approximately 10 m/s at around 0.10 s. Since the distance from the heart to the common carotid artery was roughly 17.5 cm, the times at which the mechanical vibration at 10 m/s and the incident component of the pulse wave at 5.7 m/s occurred were calculated as 78.5 and 79.2 ms after the R-wave of the ECG, respectively. As shown by the broken and dotted lines in Fig. 9(a), the PCG showed a peak at the time when these two propagation components occurred. By comparing the results among three heartbeats as shown in Fig. 9(e), the velocities estimated were similar for the incident component of the pulse wave and the mechanical vibration, and those for the reflected component of the pulse wave were also similar, which was different from those of subjects A and B; the reason is considered below.

The rise time of the relative change in the inner diameter of the blood vessel in Fig. 9(d) also corresponded to the time at which the propagation component was converted from the mechanical vibration to the incident component of the pulse wave. On the basis of the diagnostic criteria of the conventional methods, the velocity of the incident pulse wave

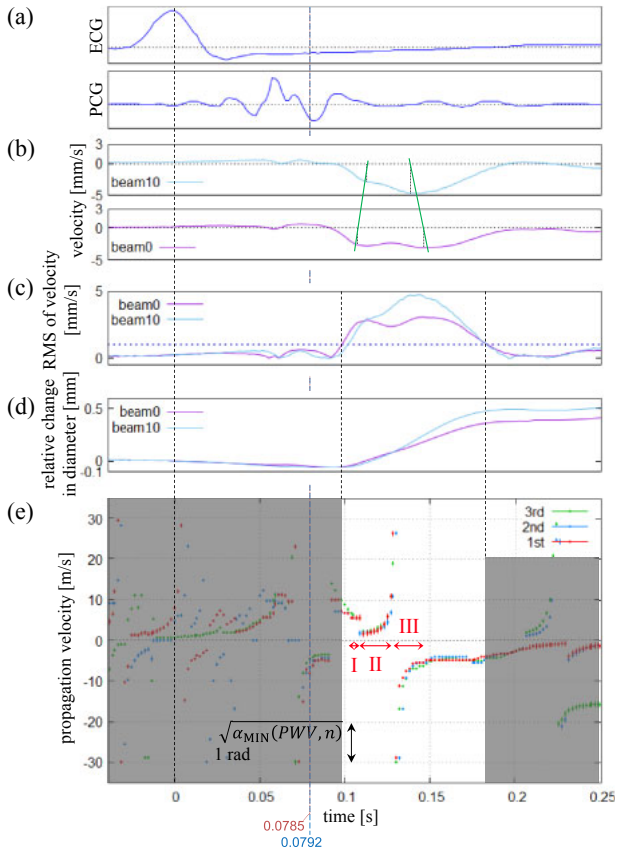

Fig. 9. (Color online) (a) ECG and PCG of subject C. (b) Velocity waveforms of small vibrations on the arterial wall of beam 0 and beam 10. (c) RMS of velocity waveforms of small vibrations on the arterial wall of beam 0 and beam 10. (d) Relative changes in the inner diameter of the blood vessel. (e) Pulse wave velocity of subject C determined by the least squares method.

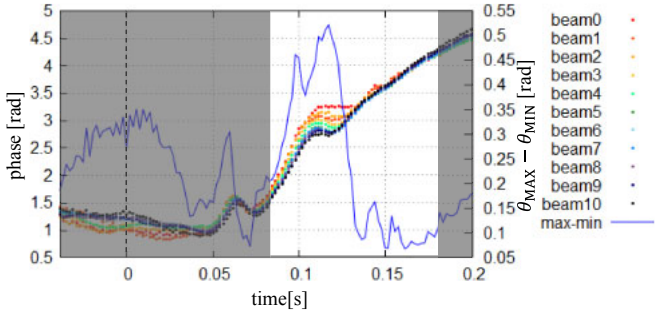

Fig. 10. (Color online) Phase waveforms of each beam and difference between the maximum phase value and the minimum phase value for subject A.

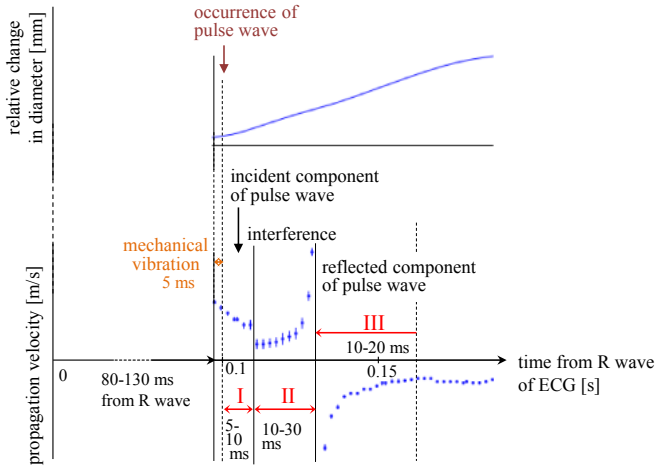

Fig. 11. (Color online) Illustration explaining the three periods of the typical propagation components.

component estimated in this study was within the normal range.

3.4 Comparison between subjects

As shown in Figs. 5(e), 7(e), and 9(e), the three propagation components, namely, the mechanical vibration and the incident and reflected components of the pulse wave were observed in all subjects immediately after the first heart sound. Therefore, the existence of these three components does not depend on the subjects. By comparing the results among heartbeats, the velocities estimated were similar for the incident component of the pulse wave and the mechanical vibration for the three subjects, while those for the reflected component of the pulse wave were different for subjects A and B. The reason is considered as follows. The maximum differences between the phase values in all beams were large for the period during which the incident components of the pulse wave were observed. On the other hand, for the period when the reflected components were observed, the maximum differences between the phase values were small. As an example, Fig. 10 shows the phase waveforms on all beams and the maximum differences between the phase values in all beams in the first heartbeat of subject A. The maximum differences between phase values at around 0.10 s when the incident component of the pulse wave was observed were larger than those at around 0.14 s during the period which the reflected component of the pulse wave was observed. Since the phase values of all beams were similar for the period when the reflected components were observed, the change in $\alpha_{\mathrm{MIN}}(PWV,n)$ with PWV was small and it was difficult to calculate PWV accurately. Thus, the velocities of the reflected component of the pulse wave were different among heartbeats.

Table I. Root of the variance $\alpha_{\mathrm{MIN}}(PWV,n)$ of the phase in the determination of PWV (in deg).

Subject	Period I	Period II	Period III
A	1.26–3.90	3.67–9.17	1.66–2.29
B	1.15–2.81	2.75–4.81	0.92–1.20
C	1.20–2.64	2.58–3.84	0.63–1.20

As illustrated in Fig. 11, the propagation components were divided into three periods for all the subjects. Period I is the period from the rise time of the inner diameter of the blood vessel to the time when the temporal change in propagation velocity has discontinuity of approximately 3 m/s. Period II is the period from the end of period I to the time when the propagation velocity changes from positive to negative. Period III is the period after the time when the propagation velocity became negative. The error bars of PWV observed in Figs. 5(e), 7(e), and 9(e) show the root of the variance in the determination of speed in Eq. (5), and Table I shows the root of the variance $\alpha(PWV,n)$ for each period for the three subjects. In all the three subjects, the values of the root of the variance $\alpha(PWV,n)$ in period II were larger than those in

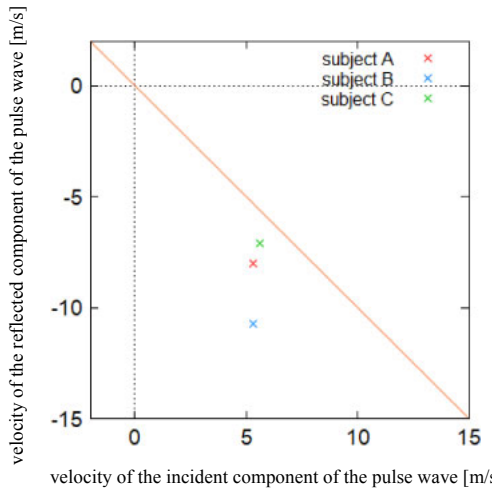

Fig. 12. (Color online) Relationship of the velocity of the incident wave component with the velocity of the reflected wave component of the three subjects.

periods I and III. The reason is maybe the interference between the incident component and the reflected component of the pulse wave in period II. The degree of this interference increases as the position becomes close to the origin of the reflection. Thus, the root of the variance $\alpha(PWV, n)$ became large.

The relationship of the velocity between the incident component and the reflected component for the three subjects is shown in Fig. 12. The reflected components of the pulse wave were calculated as faster than the incident components in all subjects. This finding is related to arterial pressure. As blood is ejected from the heart into the artery immediately after the first heart sound, the arterial pressure rises and the inner diameter of the blood vessel dilates [shown by the relative change in the inner diameter of the blood vessel waveforms in Figs. 5(d), 7(d), and 9(d)]. Thus, the inner diameter of the blood vessel at the arrival time of the reflected component of the pulse wave was larger than that at the arrival time of the incident component of the pulse wave. The modulus of elasticity of the arterial wall increases as the inner diameter of blood vessel increases, and the PWV increases. The arterial pressure at the arrival time of the reflected component of the pulse wave was higher than that at the arrival time of the incident component of the pulse wave. Thus, the *PWV* at the arrival time of the reflected component was estimated to be higher.

The distance from the measurement point to the point at which the pulse wave was reflected was calculated from using the velocities of the incident and reflected components of the pulse wave. The distances were approximately 10.6 cm for subject A, 11.7 cm for subject B, and 10.4 cm for subject C. From the estimated distance, the pulse wave would reflect from the vascular bifurcations in the arterial circle of Willis, which is at the base of the brain.

4. Conclusions

In this study, we measured the velocity of small vibrations on the arterial wall in vivo using the phase-tracking method. We applied phase unwrapping to the phase of analytic signals to obtain continuous waveforms, and then calculated the change in time of the local PWV by the least squares method. In all the three subjects, the three propagation components, namely, the mechanical vibration and the incident and reflected components of the pulse wave, were obtained immediately after the first heart sound. Furthermore, the reflected component of the pulse wave was calculated as faster than the incident component in all subjects. By the conventional method, PWV can only be calculated at a characteristic time, such as at the rise time of blood pressure waveforms.[59] By contrast, using our proposed method, it is possible to calculate the change in time of the local PWV at every time for every phase, by using the phase of analytic signals. Thus, this method may be useful for a more accurate assessment of local arteriosclerosis.

1) A. C. Burton, Physiol. Rev. **34**, 619 (1954).
2) D. H. Bergel, J. Physiol. **156**, 445 (1961).
3) T. Hirai, S. Sasayama, T. Kawasaki, and S. Yagi, Circulation **80**, 78 (1989).
4) M. A. Hajdu, D. D. Heistad, J. E. Siems, and G. L. Baumbach, Circ. Res. **66**, 1747 (1990).
5) T. I. Pynadath and D. P. Mukherjee, Atherosclerosis **26**, 311 (1977).
6) D. H. Bergel, J. Physiol. **156**, 458 (1961).
7) J. A. M. Hinke and M. L. Wilson, Am. J. Physiol. **203**, 1153 (1962).
8) B. M. Learoyd and M. G. Taylor, Circ. Res. **18**, 278 (1966).
9) D. J. Patel, W. K. Tucker, and J. S. Janicki, J. Appl. Physiol. **28**, 578 (1970).
10) D. H. Bergel, in *Biomechanics*, ed. Y. C. Fung (Prentice-Hall, Englewood Cliffs, NJ, 1972).
11) D. J. Patel, J. S. Janicki, R. N. Vaishnav, and J. T. Young, Circ. Res. **32**, 93 (1973).
12) R. H. Cox, Am. J. Physiol. **229**, 1371 (1975).
13) D. J. Mozersky, D. S. Sumner, D. E. Hokanson, and D. E. Strandness, Jr., Circulation **46**, 948 (1972).
14) T. Kawasaki, S. Sasayama, S. Yagi, T. Asakawa, and T. Hirai, Cardiovasc. Res. **21**, 678 (1987).
15) J. C. Bramwell and A. V. Hill, Proc. R. Biol. Sci. B **93**, 298 (1922).
16) J. C. Bramwell, A. V. Hill, and B. A. McSwiney, Heart **10**, 233 (1923).
17) P. Hallock, Arch. Int. Med. **54**, 770 (1934).
18) J. R. Womersley, J. Physiol. **127**, 553 (1955).
19) G. W. Morgan and W. R. Ferrante, J. Acoust. Soc. Am. **27**, 715 (1955).
20) W. W. Nichols and M. F. O'Rourke, *McDonald's Blood Flow in Arteries. Theoretical, Experimental and Clinical Principles* (Edward Arnold, London, 1998) 4th ed.
21) D. A. McDonald, J. Appl. Physiol. **24**, 73 (1968).
22) M. Anliker, M. B. Histand, and E. Ogden, Circ. Res. **23**, 539 (1968).
23) M. B. Hisland and M. Anliker, Circ. Res. **32**, 524 (1973).
24) M. G. Taylor, Phys. Med. Biol. **1**, 258 (1957).
25) U. Gessner and D. H. Bergel, IEEE Trans. Biomed. Eng. **BME-13**, 2 (1966).
26) D. A. McDonald and U. Gessner, in *Hemorheology*, ed. A. L. Copley (Pergamon, Oxford, U.K., 1968) p. 113.
27) R. H. Cox, J. Biomech. **3**, 131 (1970).
28) R. H. Cox, Circ. Res. **29**, 407 (1971).
29) N. Westerhof, P. Sipkema, G. C. Van den Bos, and G. Elzinga, Cardiovasc. Res. **6**, 648 (1972).
30) W. R. Milnor and W. W. Nichols, Circ. Res. **36**, 631 (1975).
31) W. R. Milnor and C. D. Bertram, Circ. Res. **43**, 870 (1978).
32) R. Busse, R. D. Bauer, A. Schabert, Y. Summa, and E. Wetterer, Circ. Res. **44**, 630 (1979).
33) J. K.-J. Li, J. Melbin, K. Campbell, and A. Noordergraaf, J. Biomech. **13**, 1023 (1980).
34) J. K.-J. Li, J. Melbin, R. A. Riffle, and A. Noordergraaf, Circ. Res. **49**, 442 (1981).
35) R. D. Latham, N. Westerhof, P. Sipkema, B. J. Rubal, P. Reuderink, and J. P. Murgo, Circulation **72**, 1257 (1985).
36) C. J. Mills, I. T. Gabe, J. H. Gault, D. T. Mason, J. Ross, Jr., E. Braunwald, and J. P. Shillingford, Cardiovasc. Res. **4**, 405 (1970).
37) W. Sperling, R. D. Bauer, R. Busse, H. Körner, and Th. Pasch, Pflügers Arch. Eur. J. Physiol. **355**, 217 (1975).
38) A. P. Avolio, Med. Biol. Eng. Comput. **18**, 709 (1980).
39) J. K. Li, J. Melbin, and A. Noordergraaf, Am. J. Physiol. **247**, H95 (1984).
40) K. H. Parker, C. J. H. Jones, J. R. Dawson, and D. G. Gibson, Heart Vessels **4**, 241 (1988).
41) C.-C. Lee and R. G. Mark, IEEE Trans. Biomed. Eng. **40**, 833 (1993).

42) I. T. Gabe, J. Karnell, I. G. Porje, and B. Rudewald, Acta Physiol. Scand. **61**, 73 (1964).
43) J. D. Bargainer, Circ. Res. **20**, 630 (1967).
44) T. Hayashi, Tokyo Jikei Ikadaigaku Zasshi **85**, 548 (1970) [in Japanese].
45) M. Hasegawa, Tokyo Jikei Ikadaigaku Zasshi **85**, 742 (1970) [in Japanese].
46) S. Yoshimura, M. Hasegawa, Y. Yabe, C. Arai, Y. Kashiwakura, H. Tanaka, T. Kawasaki, Y. Aizawa, M. Abe, C. Hayashi, T. Komazawa, K. Nakayama, S. Yagi, and S. Kinoshita, Kokyu to Junkan **24**, 376 (1976) [in Japanese].
47) T. Imura, K. Yamamoto, K. Kanamori, T. Mikami, and H. Yasuda, Cardiovasc. Res. **20**, 208 (1986).
48) E. D. Lehmann and R. G. Gosling, Lancet **338**, 1075 (1991).
49) M. Benthin, P. Dahl, R. Ruzicka, and K. Lindstrom, Ultrasound Med. Biol. **17**, 461 (1991).
50) P. J. Brands, J. M. Willigers, L. A. F. Ledoux, R. S. Reneman, and A. P. G. Hoeks, Ultrasound Med. Biol. **24**, 1325 (1998).
51) H. Kanai, K. Kawabe, M. Takano, R. Murata, N. Chubachi, and Y. Koiwa, Electron. Lett. **30**, 534 (1994).
52) N. Chubachi, H. Kanai, R. Murata, and Y. Koiwa, Proc. IEEE Ultrasonics Symp., 1994, **PB-9**, p. 1747.
53) A. P. Avolio, S.-G. Chen, R.-P. Wang, C.-L. Zhang, M.-F. Li, and M. F. O'Rourke, Circulation **68**, 50 (1983).
54) E. D. Lehmann, R. G. Gosling, B.-F. Langroudi, and M. G. Taylor, J. Biomed. Eng. **14**, 250 (1992).
55) E. D. Lehmann, K. D. Hopkins, and R. G. Gosling, Ultrasound Med. Biol. **19**, 683 (1993).
56) K. Takazawa, N. Tanaka, K. Takeda, F. Kurosu, and C. Ibukiyama, Hypertension **26**, 520 (1995).
57) T. Nishiya, S. Senda, K. Katakura, M. Sugawara, M. Yuba, H. Morita, H. Masugata, K. Yoshikawa, H. Yokoi, and H. Matsuo, Choonpa Igakukai **22**, 695 (1995) [in Japanese].
58) S. Laurent, J. Cockcroft, L. Bortel, P. Boutouyrie, C. Giannattasio, D. Hayoz, B. Pannier, C. Vlachopoulos, I. Wilkinson, and H. Struijker-Boudier, Eur. Heart J. **27**, 2588 (2006).
59) D. A. McDonald, *Blood Flow in Arteries* (Edward Arnold, London, 1974).
60) M. Saito, Y. Yamamoto, Y. Shibayama, M. Matsukawa, Y. Watanabe, M. Furuya, and T. Asada, Jpn. J. Appl. Phys. **50**, 07HF10 (2011).
61) H. Hasegawa, M. Sato, and T. Irie, Jpn. J. Appl. Phys. **55**, 07KF01 (2016).
62) Y. Miyachi, H. Hasegawa, and H. Kanai, Jpn. J. Appl. Phys. **54**, 07HF18 (2015).
63) H. Hasegawa, K. Hongo, and H. Kanai, J. Med. Ultrason. **40**, 91 (2013).
64) H. Kanai, M. Sato, Y. Koiwa, and N. Chubachi, IEEE Trans. Ultrason. Ferroelectr. Freq. Control **43**, 791 (1996).
65) Y. Sakai, H. Taki, and H. Kanai, Jpn. J. Appl. Phys. **55**, 07KF11 (2016).
66) A. Yamashina, H. Tomiyama, T. Arai, K. Hirose, Y. Koji, Y. Hirayama, Y. Yamamoto, and S. Hori, Hypertension Res. **26**, 615 (2003).
67) L. M. Van Bortel, S. Laurent, P. Boutouyrie, P. Chowienczyk, J. K. Cruickshank, T. De Backer, J. Filipovsky, S. Huybrechts, F. U. Mattace-Raso, A. D. Protogerou, G. Schillaci, P. Segers, S. Vermeersch, and T. Weber, J. Hypertension **30**, 445 (2012).